

Nanoarchitectonics for Hierarchical Fullerene Nanomaterials

Subjects: Materials Science, Characterization & Testing

Contributor: Lok Shrestha

Fullerenes can be regarded as simple and fundamental building blocks with mono-elemental and zero-dimensional natures, these demonstrations for hierarchical functional structures impress the high capability of the nanoarchitectonics approaches. In fact, various hierarchical structures such as cubes with nanorods, hole-in-cube assemblies, face-selectively etched assemblies, and microstructures with mesoporous frameworks are fabricated by easy fabrication protocols. The fabricated fullerene assemblies have been used for various applications including volatile organic compound sensing, microparticle catching, supercapacitors, and photoluminescence systems.

Keywords: assembly ; fullerene ; hierarchical structure ; interface ; nanoarchitectonics ; nanomaterial

1. Introduction

Nanoarchitectonics is a conceptual methodology to combine nanotechnology with other research fields such as organic chemistry, supramolecular chemistry, materials chemistry, microfabrication technology, and bio-related science [1][2]. Functional material systems are prepared from nanoscale units such as atoms, molecules, and nanomaterials through combinations and selections of building units and processes including atom/molecular manipulation, chemical transformation, self-assembly/self-organization, field-controlled organization, material processing, and bio-related treatments [3]. Because this concept is general and applicable for a wide range of materials, the nanoarchitectonics concept has been used in various research fields such as material production [4][5][6], structural fabrication [7][8][9], catalysts [10][11][12], sensing [13][14][15], devices [16][17][18], environmental usage [19][20][21], energy-related applications [22][23][24], biochemical science [25][26][27], and biomedical applications [28][29][30]. Nanoarchitectonics strategies for materials creation from fundamental units of atoms and molecules could apply to any kind of material with any desirable function [31] (Figure 1) [32].

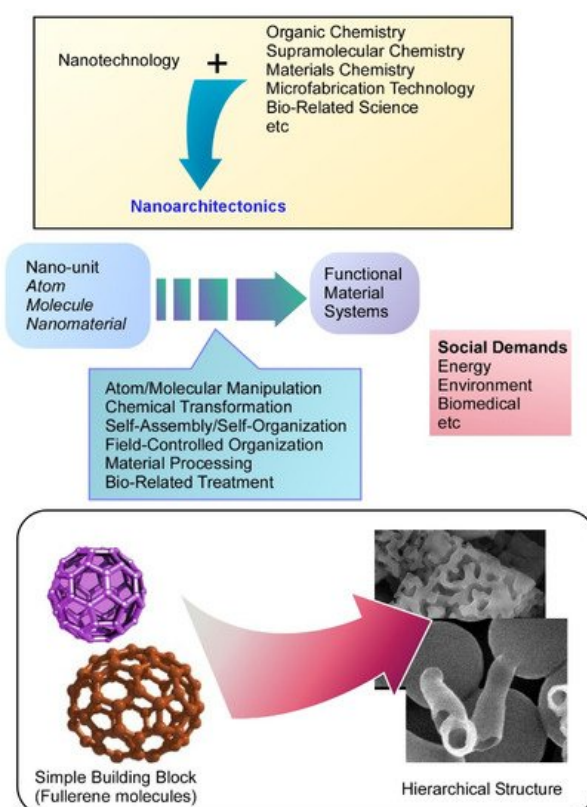


Figure 1. Nanoarchitectonics is a conceptual methodology to combine nanotechnology with other research fields, in which functional material systems are prepared from nanoscale units.

Nanoarchitectonics approaches have two distinct features. One of them is harmonized nature between contributing processes [33][34]. Unlike actions between objects at microscopic scales, the interaction between nanoscopic objects often includes uncertainties such as thermal fluctuations, statistical distributions, and quantum effects. Total effects are not always the same as a summation of individual actions. Therefore, materials productions have to be considered with the harmonization of contributing interactions rather than their simple summation. Another feature of the nanoarchitectonics approaches is advantageous features to construct asymmetric and/or hierarchical material systems [35]. Self-assembling processes are mostly driven through an energy-consume-less equilibrium. Unlike conventional self-assembling processes, the nanoarchitectonics approaches can include multiple steps where energy-consuming non-equilibrium processes are often involved. Stepwise processing and sequential treatment for materials fabrications result in the formation of materials with hierarchical structural motifs. It can be said that the nanoarchitectonics approaches are advantageous for the construction of hierarchical materials structures.

2. Hierarchically Structured Fullerene Assembly for Vapor Sensor Usage

2.1. Fullerene C₇₀ Cube for Sensing Platform for Volatile Aromatic Solvent Vapor

Bairi et al. demonstrated the preparation of hierarchically structured fullerene cubes using C₇₀ as building blocks through the liquid-liquid interfacial precipitation method (Figure 2) [36]. Structural analysis through scanning electron microscopy (SEM) and transmission electron microscopy (TEM) suggested that these cubes are composed of mesoporous fullerene C₇₀ nanorods with crystalline pore walls, which make them an excellent candidate as a receptor layer for volatile solvent detection. Detailed study of the formation mechanism highlights the importance of precise solvent engineering to control such transformation of C₇₀ fullerene cubes to hierarchically structured fullerene cubes. In this case, isopropyl alcohol was used as an additional solvent to complete this transformation process of C₇₀ fullerene cubes to hierarchically structured fullerene cubes via handshaking, followed by incubation at 25 °C for 1 h. SEM observations confirmed that isopropyl alcohol triggers the structural changes of the cubes, resulting in the formation of fullerene C₇₀ nanorods, which subsequently formed the cube surface. The high surface area and porous architecture of hierarchically structured fullerene cubes make them potential receptor materials for volatile organic compound sensing in combination with quartz crystal microbalance. These hierarchically structured fullerene cubes show excellent selectivity towards aromatic vapors over other organic volatile organic compounds due to the strong π - π interactions between host and guest. Sensitivity towards toluene is the highest among all the aromatic vapors. Additionally, sensitivity towards water vapor is very low, which is highly desirable for any kind of receptor material for gas sensing.

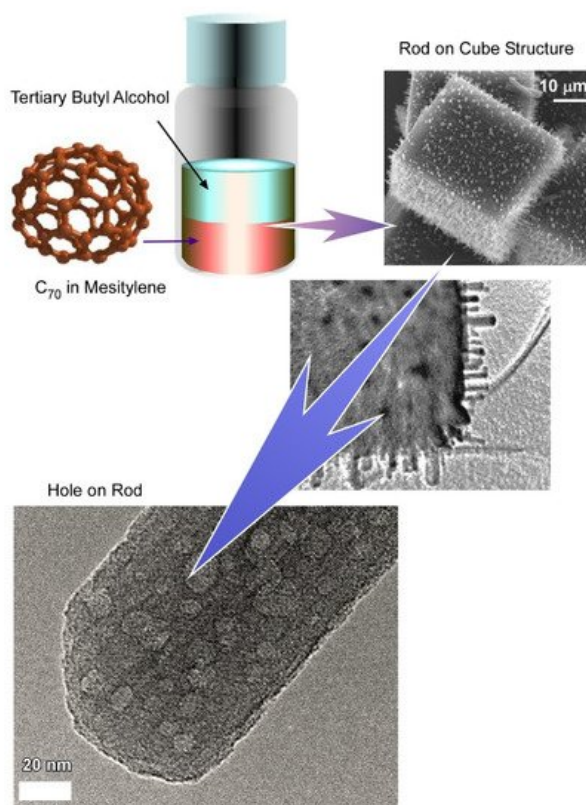


Figure 2. Preparation of hierarchically structured fullerene cubes and mesoporous fullerene C₇₀ nanorods with crystalline pore walls. Reprinted with permission from Reference [36]. Copyright 2016 American Chemical Society.

2.2. Dimension-Dependent Face-Selective Etching of Fullerene Assembly

Controlled structural modification and surface functionalization of such hierarchical fullerene microstructure is highly desirable to widen their sensing ability towards nonaromatic vapors. Additionally, conversion of hydrophobic fullerene to their hydrophilic counterpart through surface functionalization opens the possibility to use them in several biological applications. Hsieh et al. demonstrated such modification through face-selective chemical etching of fullerene assemblies (**Figure 3**) [37]. Their results showed a simple and scalable strategy for the fabrication of hollow and hierarchical fullerene nanostructures via face-selective etching of the self-assembled fullerene crystals.

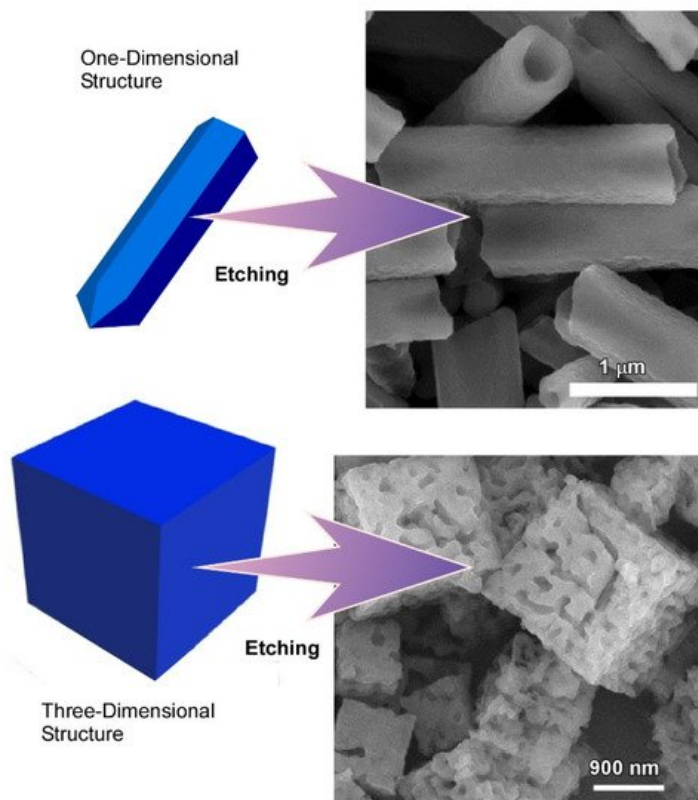


Figure 3. Formation of hollow and hierarchical fullerene nanostructures via face-selective etching of self-assembled fullerene crystals. Reprinted with permission from Reference [37]. Copyright 2020 Royal Society of Chemistry.

2.3. Bitter Melon Shaped Nanoporous Fullerene C₆₀ Assembly

As a continuation of the previous discussion, not only the surface functionality but also the shape of the fullerene hierarchical nanostructures has great importance to improve their potential application in a different field. In this regard, the combination of good solvent and poor solvent during the self-assembly of pristine fullerene via the liquid–liquid interfacial precipitation method is the determining factor to control the hierarchical structure. Furuuchi et al. demonstrated the assembly of C₆₀ into exceptional morphology called “bitter melon” shaped nanoporous C₆₀ assemblies by tuning the liquid–liquid interfacial precipitation method at room temperature (25 °C) (**Figure 4**) [38]. In this case, isopropyl alcohol was used as a poor solvent, and C₆₀ solution in dodecylbenzene as a good solvent to form a clear liquid–liquid interface. Ultrasonication and vortex mixing were applied to modify the conventional liquid–liquid interfacial precipitation method before 24 h incubation at 25 °C. XRD and high-resolution transmission electron microscopy (HRTEM) analysis confirmed the crystalline nature of the self-assembled fullerene structure. Powder XRD patterns of the as synthesized “bitter melon” shaped C₆₀ assemblies showed mixed crystal phases, including *fcc* and *hcp* phases. TEM analysis confirmed the nanoporous nature of the fullerene structure. Surface textural properties and nanoporous architectures of bitter melon shaped fullerene C₆₀ assemblies make them excellent receptor materials of quartz crystal microbalance for sensing toxic volatile organic compounds. Here also, selectivity towards aromatic solvent vapors is excellent over nonaromatic compounds due to the favorable π – π interaction. Among aromatic vapor, selectivity towards aniline is the highest.

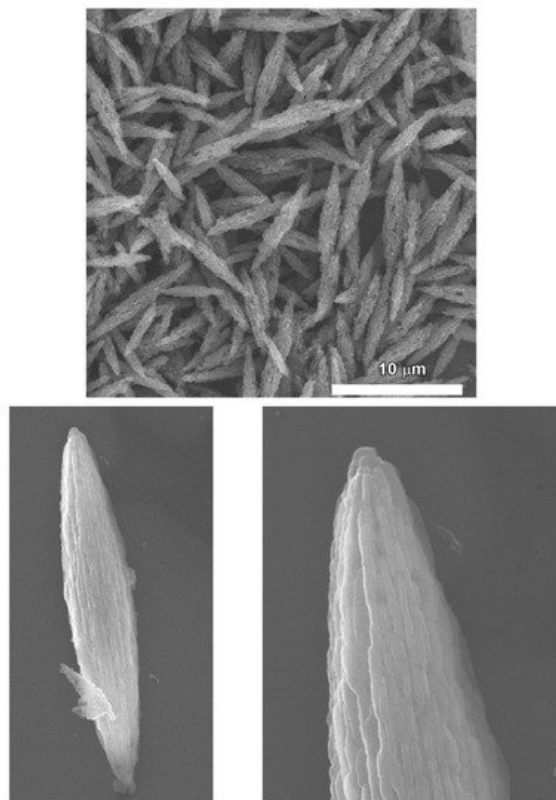


Figure 4. “Bitter melon” shaped nanoporous C_{60} assemblies prepared through the liquid–liquid interfacial precipitation method at room temperature [38].

3. Fullerene Assembly with Microscopic Recognition Capability

3.1. Hole-in-Cube Fullerene Assembly with Microscopic Recognition Capability

Bairi et al. demonstrated the fabrication of a C_{70} cube with an open hole on each face of the cube through controlled self-assembly at the liquid–liquid interface (**Figure 5**) [39]. Additionally, it was established that the process to close and open the holes can be done purposefully. Fullerene C_{70} cubes with open or closed holes were produced by the dynamic liquid–liquid interfacial precipitation method at 25 °C using mesitylene as a good solvent and tertiary butyl alcohol as a poor solvent followed by 24 h incubation under 25 °C. The formation mechanism of such an open hole cube is different from the previously discussed solvent or chemical etching mechanisms. Detailed structural analysis via cross-section SEM confirmed that the holes are not hollow through. Additionally, TEM images of fullerene assemblies formed just after the mixing of C_{70} -mesitylene with tertiary butyl alcohol confirmed the formation of a smaller cube with no holes. It was suggested from this observation that the open hole formation is not driven by the solvent etching mechanism, but rather the growth of open hole cubes involves a two-step process including a solid core formation at the first step followed by slow growth to the final open hole cube formation. In the second step, concentration depletion and the different reactivity of the corner, as well as the edges, play important roles to form such a uniform open hole cube. This observation is in line with the formation mechanism of the closed hole cube. When the mesitylene/tertiary butyl alcohol ratio is fixed at 1:2, the C_{70} concentration is below the critical concentration level to form the new core. Therefore, C_{70} molecules tend to grow over each face of the open hole cube to form the closed hole cube.

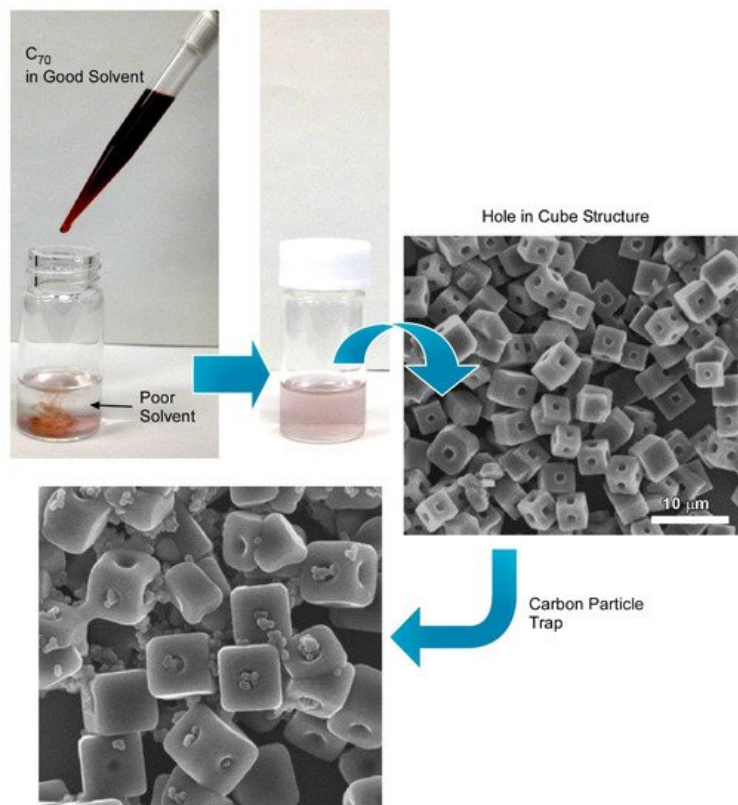


Figure 5. Fabrication of C_{70} cube with open hole on each face of the cube (hole-in-cube structure) through controlled self-assembly at the liquid–liquid interface and trapping capability for carbon particles. Reprinted with permission from Reference [39]. Copyright 2017 American Chemical Society.

3.2. Fullerene Microhorns with Microscopic Recognition Properties

Recently, Tang et al. demonstrated the fabrication of fullerene microstructures with a hollow framework from a mixture of C_{60} and C_{70} based on the dynamic liquid–liquid interfacial precipitation method (**Figure 6**) [40]. Additionally, considering the different crystalline phases and solubility of C_{60} and C_{70} and precise solvent engineering, they can transform the microstructure into unique conical-shaped fullerene microhorns. A C_{60} and C_{70} fullerene mixture with a 4:1 volume ratio was used in mesitylene as a good solvent. A mixed fullerene microtube was fabricated by the dynamic liquid–liquid interfacial precipitation method using tertiary butyl alcohol as a poor solvent. The overall reaction was very fast and completed in a few seconds after the addition of the fullerene fixture into the poor solvent. Details analysis suggests that the mixing ratio of fullerene C_{60} and C_{70} plays an important role to control the formation of the microtube. Interestingly, the microtube formation of fullerene C_{70} is not possible due to their crystal packing. However, with the help of fullerene C_{60} , fullerene C_{70} was forced to form the microtube through hexagonal closed packing. Fullerene microtube-to-microhorn transformation was accomplished by precise solvent engineering. Then, a mesitylene/tertiary butyl alcohol (volume ratio of 1:3) solvent mixture was used to wash the microtube to form the perfectly homogeneous microhorn. Interestingly, there was no change in crystallinity of the microhorn, which suggests that the process of such morphological transformation is fully dominated by the physical changes. Additionally, such solvent engineering helps us to generate a nanoporous architecture inside the microhorn.

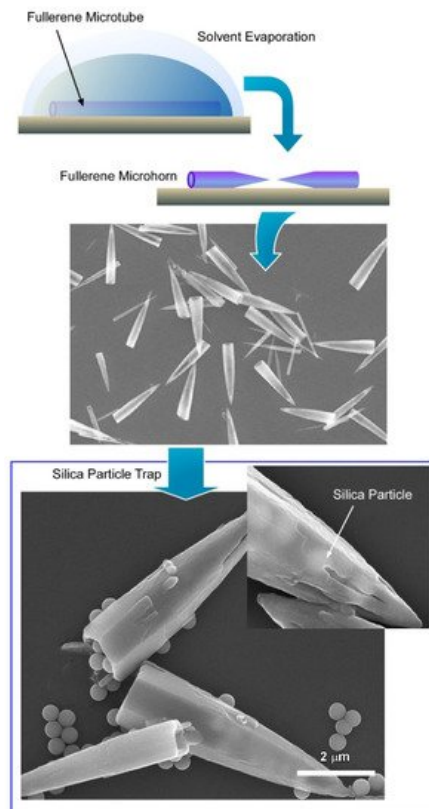


Figure 6. Formation of conical-shaped fullerene microhorn from fullerene microtube and trapping behavior of silica particles. Reprinted with permission from Reference [40]. Copyright 2019 American Chemical Society.

4. Fullerene Microstructure with Mesoporous Framework for Advanced Function

4.1. Mesoporous Fullerene C₇₀ Cube with Enhanced Photoluminescence Property

Bairi et al. have recently demonstrated one such novel piece of work, which includes the formation of mesoporous fullerene C₇₀ cubes with highly crystalline frameworks with excellent photoluminescence properties [41]. Crystalline fullerene cubes with sharp edges were fabricated by the ultrasound liquid–liquid interfacial precipitation method from tertiary butyl alcohol as a poor solvent and a solution of C₇₀ in mesitylene as a good solvent at 25 °C. A good solvent to poor solvent ratio is one of the important parameters to control the desired morphology, and here in this case it was 1:5. After the preparation of the fullerene cube, the mother liquor was stirred at 300 rpm for 72 h at 75 °C and then drop-casted on a silicon wafer and dried at 80 °C to prepared the mesoporous crystalline fullerene cube. An adsorption isotherm confirmed the formation of mesopore inside the fullerene cube, as the surface area of the mesoporous structure was higher than that of the fullerene cube. Crystal structure analysis via XRD confirmed that the as-synthesized fullerene cube contained the simple cube packing, whereas mesoporous has a mixed crystal phase with a simple cube and hexagonal closed pack. This phenomenon can be attributed to the entrapped solvent molecules, which change the crystal packing of C₇₀ and reducing the crystal symmetry. Photoluminescence properties of mesoporous fullerene cubes are improved by such crystallographic modification, which can be confirmed from the comparison of photoluminescence spectra of pristine C₇₀, fullerene cubes, and mesoporous fullerene cubes. It is worth noticing that for π -conjugated molecules, photoluminescence intensity is quenched in the solid-state. However, the photoluminescence intensity of mesoporous fullerene cubes is higher in the solid-state, which indicates the importance of such structural and crystalline framework modification.

4.2. Mesoporous Carbon Cubes for Supercapacitors

During the last three decades, researchers have given enormous efforts to finding suitable mesoporous materials for charge storage applications [42][43][44]. Carbon-based materials with mesoporous architectures are supposed to be the best materials for such charge storage properties [45][46][47]. However, unwanted surface functionality and poor electrochemical conductivity of such carbon materials have to be addressed to improve their performance. Fullerene C₆₀ or C₇₀ is a π -conjugated molecule and readily self-assembles to form a homogeneous shape-controlled microstructure. Recently, researchers have focused on these dimensionally-controlled fullerene assemblies as an exceptional source of π -electron-rich carbon materials. Such extended conjugated π -systems with high surface areas and mesoporous frameworks will be advantageous for energy storage applications such as supercapacitors, battery, etc. [48][49][50].

Bairi et al. demonstrated the direct transformation of porous crystalline fullerene C_{70} cubes into mesoporous carbon cubes that possess a very high specific surface area [51]. Synthesis of a porous crystalline C_{70} cube was done by the liquid–liquid interfacial precipitation method followed by mild heat treatment at 70 °C. XRD and TEM analysis confirmed the crystalline framework of the C_{70} cube. Conversion of porous crystalline fullerene C_{70} cubes to high surface area mesoporous carbon cubes was performed by high-temperature heat treatment (900 °C) under a continuous flow of N_2 gas in a tube furnace. A nitrogen adsorption isotherm confirmed the formation of a mesoporous architecture with a narrow pore size distribution. The Brunauer–Emmett–Teller surface area of the mesoporous carbon cube was very high at ca. $642.6 \text{ m}^2 \text{ g}^{-1}$, which is almost 14 times higher than that of the porous crystalline fullerene cube (ca. $47.7 \text{ m}^2 \text{ g}^{-1}$). Therefore, high-temperature heat treatment is an essential step for such a large improvement of specific surface area. Pore size analysis by Barrett–Joyner–Halenda and the non-local density functional theory method confirmed the presence of both micropores and mesopores. The average pore size of the obtained carbon cube was 3.44 nm with a high pore volume of $0.367 \text{ cm}^3 \text{ g}^{-1}$. XRD and Raman analysis of the obtained carbon cube confirmed the graphitic nature of carbon.

4.3. Quasi Two-Dimensional Mesoporous Carbon Microbelts for Supercapacitors

Electrochemical charge storage is highly dependent on the effective surface area accessible to the electrolyte ions. Therefore, it is very important to change the morphology of the fullerene-derived carbon to obtain maximum charge storage capacity. Here, fullerenes offer a great opportunity, as they can form almost any kind of morphology starting from one-dimensional rod to two-dimensional sheet to three-dimensional cube through the supramolecular assembly. Studies on charge storage mechanisms suggest that the sheet-like structure shows great performance.

Recently, Tang, et al. reported a novel method for fabrication of two-dimensional fullerene microbelts, which can be transferred to mesoporous carbon with the retention of their original sheet-like structure (Figure 7) [52].

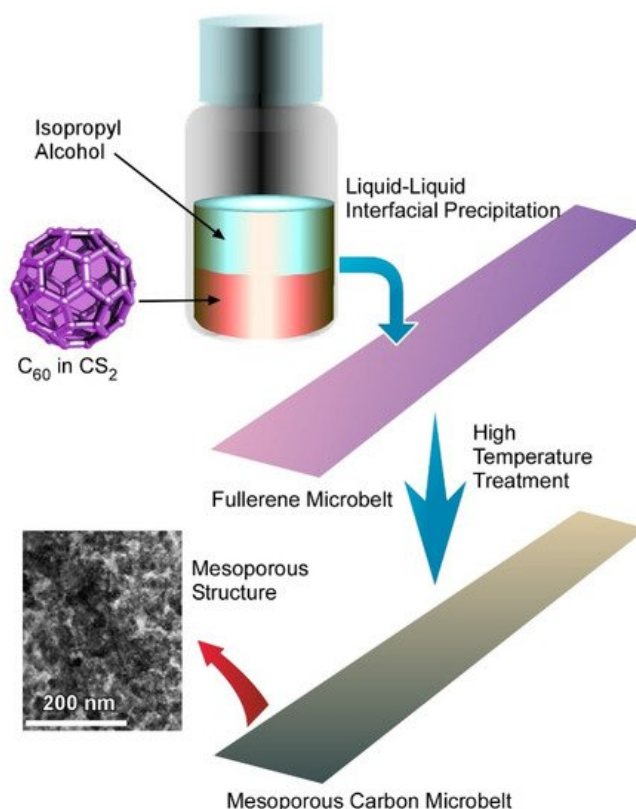


Figure 7. Fabrication of two-dimensional fullerene microbelts through transformation of fullerene assembly to mesoporous carbon with retention of their original sheet-like structure. Reprinted with permission from Reference [52]. Copyright 2017 American Chemical Society.

References

1. Ariga, K. Nanoarchitectonics Revolution and Evolution: From Small Science to Big Technology. *Small Sci.* 2020, 1, 2000032.
2. Ariga, K. Nanoarchitectonics at Interfaces for Regulations of Biorelated Phenomena: Small Structures with Big Effects. *Small Struct.* 2021, 2, 2100006.

3. Ariga, K.; Li, J.; Fei, J.; Ji, Q.; Hill, J. Nanoarchitectonics for Dynamic Functional Materials from Atomic-/Molecular-Level Manipulation to Macroscopic Action. *Adv. Mater.* 2015, 28, 1251–1286.
4. Sang, Y.; Liu, M. Nanoarchitectonics through supramolecular gelation: Formation and switching of diverse nanostructures. *Mol. Syst. Des. Eng.* 2018, 4, 11–28.
5. Tirayaphanitchkul, C.; Imwiset, K.; Ogawa, M. Nanoarchitectonics through Organic Modification of Oxide Based Layered Materials; Concepts, Methods and Functions. *Bull. Chem. Soc. Jpn.* 2021, 94, 678–693.
6. Liu, X.; Chen, T.; Gong, Y.; Li, C.; Niu, L.; Xu, S.; Xu, X.; Pan, L.; Shapter, J.G.; Yamauchi, Y.; et al. Light-conversion phosphor nanoarchitectonics for improved light harvesting in sensitized solar cells. *J. Photochem. Photobiol. C Photochem. Rev.* 2021, 47, 100404.
7. Ramanathan, M.; Shrestha, L.; Mori, T.; Ji, Q.; Hill, J.; Ariga, K. Amphiphile nanoarchitectonics: From basic physical chemistry to advanced applications. *Phys. Chem. Chem. Phys.* 2013, 15, 10580–10611.
8. Ariga, K.; Mori, T.; Kitao, T.; Uemura, T. Supramolecular chiral nanoarchitectonics. *Adv. Mater.* 2020, 32, 1905657.
9. Cheng, P.; Wang, C.; Kaneti, Y.V.; Eguchi, M.; Lin, J.; Yamauchi, Y.; Na, J. Practical MOF Nanoarchitectonics: New Strategies for Enhancing the Processability of MOFs for Practical Applications. *Langmuir* 2020, 36, 4231–4249.
10. Abe, H.; Liu, J.; Ariga, K. Catalytic nanoarchitectonics for environmentally compatible energy generation. *Mater. Today* 2015, 19, 12–18.
11. Kumari, N.; Kumar, A.; Krishnan, V. Ultrathin Au–Ag Heterojunctions on Nanoarchitectonics Based Biomimetic Substrates for Dip Catalysis. *J. Inorg. Organomet. Polym. Mater.* 2021, 31, 1954–1966.
12. Chen, G.; Sciortino, F.; Ariga, K. Atomic Nanoarchitectonics for Catalysis. *Adv. Mater. Interfaces* 2020, 8, 2001395.
13. Ishihara, S.; Labuta, J.; Van Rossom, W.; Ishikawa, D.; Minami, K.; Hill, J.; Ariga, K. Porphyrin-based sensor nanoarchitectonics in diverse physical detection modes. *Phys. Chem. Chem. Phys.* 2014, 16, 9713–9746.
14. Pandeeswar, M.; Senanayak, S.P.; Govindaraju, T. Nanoarchitectonics of Small Molecule and DNA for Ultrasensitive Detection of Mercury. *ACS Appl. Mater. Interfaces* 2016, 8, 30362–30371.
15. Liu, J.; Zhou, H.; Yang, W.; Ariga, K. Soft Nanoarchitectonics for Enantioselective Biosensing. *Accounts Chem. Res.* 2020, 53, 644–653.
16. Ariga, K.; Ji, Q.; Mori, T.; Naito, M.; Yamauchi, Y.; Abe, H.; Hill, J. Enzyme nanoarchitectonics: Organization and device application. *Chem. Soc. Rev.* 2013, 42, 6322–6345.
17. Ariga, K.; Ito, M.; Mori, T.; Watanabe, S.; Takeya, J. Atom/molecular nanoarchitectonics for devices and related applications. *Nano Today* 2019, 28, 100762.
18. Giussi, J.M.; Cortez, M.L.; Marmisollé, W.A.; Azzaroni, O. Practical use of polymer brushes in sustainable energy applications: Interfacial nanoarchitectonics for high-efficiency devices. *Chem. Soc. Rev.* 2019, 48, 814–849.
19. Ariga, K.; Ishihara, S.; Abe, H.; Li, M.; Hill, J. Materials nanoarchitectonics for environmental remediation and sensing. *J. Mater. Chem.* 2011, 22, 2369–2377.
20. Pham, T.; Qamar, A.; Dinh, T.; Masud, M.K.; Rais-Zadeh, M.; Senesky, D.G.; Yamauchi, Y.; Nguyen, N.; Phan, H. Nanoarchitectonics for Wide Bandgap Semiconductor Nanowires: Toward the Next Generation of Nanoelectromechanical Systems for Environmental Monitoring. *Adv. Sci.* 2020, 7, 2001294.
21. Ariga, K. Nanoarchitectonics Can Save Our Planet: Nanoarchitectonics for Energy and Environment. *J. Inorg. Organomet. Polym. Mater.* 2021, 31, 2243–2244.
22. Kim, J.; Kim, J.H.; Ariga, K. Redox-active polymers for energy storage nanoarchitectonics. *Joule* 2017, 1, 739–768.
23. Xu, J.; Zhang, J.; Zhang, W.; Lee, C.-S. Interlayer Nanoarchitectonics of Two-Dimensional Transition-Metal Dichalcogenides Nanosheets for Energy Storage and Conversion Applications. *Adv. Energy Mater.* 2017, 7, 1700571.
24. Huang, H.; Yan, M.; Yang, C.; He, H.; Jiang, Q.; Yang, L.; Lu, Z.; Sun, Z.; Xu, X.; Bando, Y.; et al. Graphene Nanoarchitectonics: Recent Advances in Graphene-Based Electrocatalysts for Hydrogen Evolution Reaction. *Adv. Mater.* 2019, 31, e1903415.
25. Stulz, E. Nanoarchitectonics with Porphyrin Functionalized DNA. *Accounts Chem. Res.* 2017, 50, 823–831.
26. Liang, X.; Li, L.; Tang, J.; Komiyama, M.; Ariga, K. Dynamism of Supramolecular DNA/RNA Nanoarchitectonics: From Interlocked Structures to Molecular Machines. *Bull. Chem. Soc. Jpn.* 2020, 93, 581–603.
27. Ariga, K.; Fakhrullin, R. Nanoarchitectonics on living cells. *RSC Adv.* 2021, 11, 18898–18914.
28. Ariga, K.; Leong, D.T.; Mori, T. Nanoarchitectonics for Hybrid and Related Materials for Bio-Oriented Applications. *Adv. Funct. Mater.* 2017, 28, 1702905.

29. Zhao, L.; Zou, Q.; Yan, X. Self-Assembling Peptide-Based Nanoarchitectonics. *Bull. Chem. Soc. Jpn.* 2019, 92, 70–79.
30. Ariga, K.; Tsai, K.-C.; Shrestha, L.K.; Hsu, S.-H. Life science nanoarchitectonics at interfaces. *Mater. Chem. Front.* 2020, 5, 1018–1032.
31. Ariga, K. There's still plenty of room at the bottom. *Chem. World* 2021, 18, 5.
32. Ariga, K.; Yamauchi, Y. Nanoarchitectonics from Atom to Life. *Chem. Asian J.* 2020, 15, 718–728.
33. Aono, M.; Ariga, K. The Way to Nanoarchitectonics and the Way of Nanoarchitectonics. *Adv. Mater.* 2015, 28, 989–992.
34. Ariga, K. Nanoarchitectonics: A navigator from materials to life. *Mater. Chem. Front.* 2016, 1, 208–211.
35. Ariga, K.; Jia, X.; Song, J.; Hill, J.P.; Leong, D.T.; Jia, Y.; Li, J. Nanoarchitectonics beyond Self-Assembly: Challenges to Create Bio-Like Hierarchic Organization. *Angew. Chem. Int. Ed.* 2020, 59, 15424–15446.
36. Bairi, P.; Minami, K.; Nakanishi, W.; Hill, J.; Ariga, K.; Shrestha, L. Hierarchically Structured Fullerene C70 Cube for Sensing Volatile Aromatic Solvent Vapors. *ACS Nano* 2016, 10, 6631–6637.
37. Hsieh, C.-T.; Hsu, S.-H.; Maji, S.; Chahal, M.K.K.; Song, J.; Hill, J.P.; Ariga, K.; Shrestha, L.K. Post-assembly dimension-dependent face-selective etching of fullerene crystals. *Mater. Horiz.* 2019, 7, 787–795.
38. Furuuchi, N.; Shrestha, R.G.; Yamashita, Y.; Hirao, T.; Ariga, K.; Shrestha, L.K. Self-Assembled Fullerene Crystals as Excellent Aromatic Vapor Sensors. *Sensors* 2019, 19, 267.
39. Bairi, P.; Minami, K.; Hill, J.P.; Ariga, K.; Shrestha, L.K. Intentional Closing/Opening of “Hole-in-Cube” Fullerene Crystals with Microscopic Recognition Properties. *ACS Nano* 2017, 11, 7790–7796.
40. Tang, Q.; Maji, S.; Jiang, B.; Sun, J.; Zhao, W.; Hill, J.P.; Ariga, K.; Fuchs, H.; Ji, Q.; Shrestha, L.K. Manipulating the Structural Transformation of Fullerene Microtubes to Fullerene Microhorns Having Microscopic Recognition Properties. *ACS Nano* 2019, 13, 14005–14012.
41. Bairi, P.; Tsuruoka, T.; Acharya, S.; Ji, Q.; Hill, J.P.; Ariga, K.; Yamauchi, Y.; Shrestha, L. Mesoporous fullerene C70 cubes with highly crystalline frameworks and unusually enhanced photoluminescence properties. *Mater. Horiz.* 2018, 5, 285–290.
42. Wang, Q.; Zhang, Y.; Jiang, H.; Li, X.; Cheng, Y.; Meng, C. Designed mesoporous hollow sphere architecture metal (Mn, Co, Ni) silicate: A potential electrode material for flexible all solid-state asymmetric supercapacitor. *Chem. Eng. J.* 2019, 362, 818–829.
43. Saito, Y.; Ashizawa, M.; Matsumoto, H. Mesoporous Hydrated Graphene Nanoribbon Electrodes for Efficient Supercapacitors: Effect of Nanoribbon Dispersion on Pore Structure. *Bull. Chem. Soc. Jpn.* 2020, 93, 1268–1274.
44. Li, Y.; Henzie, J.; Park, T.; Wang, J.; Young, C.; Xie, H.; Yi, J.W.; Li, J.; Kim, M.; Kim, J.; et al. Fabrication of Flexible Microsupercapacitors with Binder-Free ZIF-8 Derived Carbon Films via Electrophoretic Deposition. *Bull. Chem. Soc. Jpn.* 2020, 93, 176–181.
45. Nomura, K.; Nishihara, H.; Kobayashi, N.; Asada, T.; Kyotani, T. 4.4 V supercapacitors based on super-stable mesoporous carbon sheet made of edge-free graphene walls. *Energy Environ. Sci.* 2019, 12, 1542–1549.
46. Kim, G.; Shiraki, T.; Fujigaya, T. Thermal Conversion of Triazine-Based Covalent Organic Frameworks to Nitrogen-Doped Nanoporous Carbons and Their Capacitor Performance. *Bull. Chem. Soc. Jpn.* 2020, 93, 414–420.
47. Shrestha, R.L.; Chaudhary, R.; Shrestha, R.G.; Shrestha, T.; Maji, S.; Ariga, K.; Shrestha, L.K. Washnut Seed-Derived Ultrahigh Surface Area Nanoporous Carbons as High Rate Performance Electrode Material for Supercapacitors. *Bull. Chem. Soc. Jpn.* 2021, 94, 565–572.
48. Shrestha, L.; Shrestha, R.G.; Yamauchi, Y.; Hill, J.; Nishimura, T.; Miyazawa, K.; Kawai, T.; Okada, S.; Wakabayashi, K.; Ariga, K. Nanoporous Carbon Tubes from Fullerene Crystals as the π -Electron Carbon Source. *Angew. Chem. Int. Ed.* 2014, 54, 951–955.
49. Sengottaiyan, C.; Jayavel, R.; Shrestha, R.G.; Subramani, T.; Maji, S.; Kim, J.H.; Hill, J.P.; Ariga, K.; Shrestha, L. Indium Oxide/Carbon Nanotube/Reduced Graphene Oxide Ternary Nanocomposite with Enhanced Electrochemical Supercapacitance. *Bull. Chem. Soc. Jpn.* 2019, 92, 521–528.
50. Baskar, A.V.; Ruban, A.M.; Davidraj, J.M.; Singh, G.; Al-Muhtaseb, A.H.; Lee, J.M.; Yi, J.; Vinu, A. Single-Step Synthesis of 2D Mesoporous C60/Carbon Hybrids for Supercapacitor and Li-Ion Battery Applications. *Bull. Chem. Soc. Jpn.* 2021, 94, 133–140.
51. Bairi, P.; Maji, S.; Hill, J.P.; Kim, J.H.; Ariga, K.; Shrestha, L.K. Mesoporous carbon cubes derived from fullerene crystals as a high rate performance electrode material for supercapacitors. *J. Mater. Chem. A* 2019, 7, 12654–12660.
52. Tang, Q.; Bairi, P.; Shrestha, R.G.; Hill, J.P.; Ariga, K.; Zeng, H.; Ji, Q.; Shrestha, L.K. Quasi 2D Mesoporous Carbon Microbelts Derived from Fullerene Crystals as an Electrode Material for Electrochemical Supercapacitors. *ACS Appl. Mater. Sci.* 2019, 11, 10100–10108.

Retrieved from <https://encyclopedia.pub/entry/history/show/32936>